Parallel simulation of rock deformation processes

Yevhen Tiurin[1][0000-0001-8362-9223], Antonina Andrieieva[1][0000-0002-0361-5436]

[1]Donetsk National Technical University, Shybankova sq., 2, Pokrovsk, 85300, Ukraine
yevhen.tiurin@donntu.edu.ua, antonina.andrieieva@donntu.edu.ua

Abstract. This paper enlightens the simulation of rock deformation processes on multicore processing. For mines rock deformation processes affect gas emissions and its prediction is an important research and modeling task. In this paper, the parallel architectures OpenMP and MPI are used. The results show the modeling time of OpenMP and MPI are better than the serial programming when the number of grids is given more than 400 points.

Keywords. Parallel simulation, SIMD, MIMD, deformation process, rock deformation.

1 Introduction

With the transition of mining operations to the region of great depths (significantly lower than the gas weathering zone), external and internal factors related to the coal layer, which cause the occurrence of GDH are likely to change. In this aspect, the most careful attention should be paid to the geomechanical processes occurring in the near-bottom part of the coal layer.

In various studies of the stress state of a rock mass, as a rule, the mass is considered as an elastic medium. The stress concentration in the edge of the layer, located at depths of more than about 300 - 400 m, leads to the formation of an inelastic deformation zone [1, 2, 3, 4, 5]. However, taking into account the physical and mechanical properties of the coal layer, the geomechanical, chemical and gas-dynamic processes occurring in this zone, besides plastic deformation, brittle destruction of the rock and deformation of the genetic return also occur. It will be generally fair to consider this zone as a zone of inelastic deformations.

In the process of coal mining in the bottom, the boundary of the zone of inelastic deformation moves deep into the massif and the bottom-hole part of the coal layer is extracted into the mine.

Over time and under the influence of existing stresses, the equilibrium state of the bottom-hole part of the coal layer can be disturbed, and often it happens. The interaction of these factors, and the physicomechanical properties of the layer and host rocks, leads to a critical state of coal in the near-bottom part of the layer and its natural softening and destruction.

It should be noted that the destruction of the edge of the coal layer occurs during unloading due to excavation of the next strip (part) of coal in the lava. The condition

on the destruction of a solids not with an increase or prolonged exposure to normal or shear stresses, but with unloading, was noted back in the 40-50s of the last century by the American scientist P. Bridgman [6, 7].

Over time, numerous experimental studies have proved the fundamental impossibility of the origin and occurrence of GDH in the unloaded part of the outburst hazardous layer below the gas weathering zone, at great depths.

The formation and development of the zone of inelastic deformations in the boundary part of the layer always occurs during stress redistribution. This part of the layer is characterized by reduced tension and, consequently, an increased tendency to gas recovery - gas evolution. With an increase in the depth of mining operations, and consequently, an increase in rock pressure, the processes of destruction of the edge part are undoubtedly intensified.

The conditions on the non-outburst hazard of the edge of the outburst layer formed the basis of many methods for predicting, preventing GDH and monitoring their effectiveness, which were included in the new standard of the «Ministry of Industry of Ukraine» [8].

Substantial growth below the gas weathering zones of the extraction strains was determined, which allows, in this regard, to produce in it a more productive, controlled extraction of coal from the outburst hazardous layer without causing sudden outbursts.

On this basis, rock deformation processes affect gas emissions and its prediction is an important research and modeling task.

2   Mathematical description

To simulate the deformation process, a system of equations of mechanics including the equations:

- continuity

$$\rho + \rho u_{i,j} = 0 \tag{1}$$

- movement

$$\sigma_{ji,i} + \rho F_j = \rho \dot{u}_j. \tag{2}$$

Here:

ρ – the density of the material;

u_j – the components of the velocity vector;

$\sigma_{j,i}$ – the components of the Cauchy stress tensor;

F_j – mass forces.

Here ρ is the density of the material; u_j are the components of the velocity vector; $\sigma_{j,i}$ are the components of the Cauchy stress tensor; F_j - mass forces; the dot above means the tiem derivative, the index after the decimal point means the corresponding coordinate derivative. The system of equations is closed by defining relations that specify the behavior of the medium during deformation. When writing the defining relations, the decomposition of the stress tensor into the spherical and deviator parts is used:

$$\sigma_{j,i} = -\sigma\delta_{j,i} + S_{j,i} \qquad (3)$$

Where:
$-\sigma$ – average pressure;

$S_{j,i}$ – stress tensor deviator components:

$\delta_{j,i}$ – Kronecker symbol.

Before the onset of a plastic state, the rates of stress and strain changes are related by a hypoelastic law:

$$\frac{DS_{j,i}}{D_t} = 2\mu_0(\dot{\varepsilon}_{j,i} - \frac{1}{3}\dot{\varepsilon}_{nn}\delta_{j,i}), \qquad (4)$$

$$\frac{DS_{j,i}}{D_t} = \dot{S}_{j,i} - S_{ni}\dot{\omega}_{nj} - S_{nj}\dot{\omega}_{n,j}, \qquad (5)$$

$$\dot{\sigma} = -K\frac{\dot{V}}{V}. \qquad (6)$$

where K и μ – compression and shear modules, respectively. The components of the strain rate tensor $\dot{\varepsilon}_{j,i}$ rotational speed tensor components $\dot{\omega}_{j,i}$ are determined from the relations:

$$\dot{\varepsilon}_{j,i} = \frac{1}{2}(u_{j,i} + u_{i,j}), \qquad (7)$$

$$\dot{\omega}_{j,i} = \frac{1}{2}(u_{j,i} - u_{i,j}). \qquad (8)$$

It is accepted that the deformation consists of elastic e and plastic p parts. For strain rate, this decomposition is written as:

$$\dot{\varepsilon} = \dot{\varepsilon}^e + \dot{\varepsilon}^p. \qquad (9)$$

Plastic deformation is determined in accordance with the equation of the limiting surface and plastic potential:

$$f(\sigma_{j,i}, \varepsilon_{j,i}^p) = 0, \tag{10}$$

$$g(\sigma_{j,i}, \varepsilon_{j,i}^p) = 0, \tag{11}$$

$$d\varepsilon_{j,i}^p = d\lambda \frac{\partial g}{\partial \sigma_{j,i}}, \tag{12}$$

Where:

f – load surface (function) equation;

g – plastic potential;

$d\lambda$ - determined during deformation from the condition of plasticity;

$\varepsilon_{j,i}^p$ – components of plastic (inelastic) deformation.

Limiting surface (fig. 1) in the area of shear deformation in the pressure range $\sigma_j \leq \sigma \leq \sigma_0$ described by the equation

$$f_1(\sigma, \tau) = \tau - \alpha\sigma - c \tag{13}$$

and with pressures $\sigma > \sigma_0$ – by the equation

$$f_2(\sigma, \tau) = \frac{(\sigma - \sigma_0)^2}{a^2} + \frac{\tau^2}{b^2} - 1 = 0. \tag{14}$$

Here $\alpha = \alpha(e^n, \sigma)$, $c = c(e^n, \sigma)$ – coefficients of internal friction and adhesion, $\tau = (S_{j,i} S_{i,j} / 2)^{\frac{1}{2}}$ – second stress deviator invariant, σ_t – tear strength, σ_0 – threshold pressure at which material compaction begins, $a = \sigma_1 - \sigma_0$, $b = c + \alpha\sigma_0$.

The normal to the plastic potential $g = \tau - \Lambda\sigma$ determines the direction of plastic strain increments, where Λ – is the dilatancy coefficient.

It is accepted that during the development of inelastic deformation, a change in the surface of the limiting state occurs, as well as damage accumulation, which macroscopically manifests itself in a change in volume, i.e., in medium dilatancy. The hardening of the medium is described by the relation

$$c(\gamma^p) = c_0[1 + h(A(\gamma^p) - D(\gamma^p))] \tag{15}$$

where h – hardening coefficient, $d\gamma^p = 2((de_{j,i})^{2p}/2)^{\frac{1}{2}}$ shear plastic strain rate, γ^* – critical deformation, after which degradation of the material predominates. To account for hardening, a linear relationship $A\gamma(\gamma^p) = 2\gamma^2/\gamma$ and quadratic - to take into account softening (accumulation of damage)

$$D(\gamma^p) = (\gamma^p/\gamma) \tag{16}$$

The effect of pressure on the limiting strain that the material can withstand before softening begins is taken into account by the expression:

$$\gamma^* = \gamma_0^*(1 + w\sigma/\sigma^*) \tag{17}$$

where γ_0^* – plastic deformation of the onset of fracture in the absence of compressive (restraining) pressure; w and σ^* – parameters. This method made it possible to describe the transition from brittle to "viscous" behavior with increasing pressure [9].

Two-dimensional deformation processes are considered for conditions of plane deformation when $u_z = 0, \dot{\varepsilon}_{xz} = \dot{\varepsilon}_{yz} = \dot{\varepsilon}_{zz} = 0.$.

To simulate the process of rock deformation, the approach [10] was used, which is based on solving the equations of dynamics of an elastic-plastic medium using an explicit numerical scheme [11].
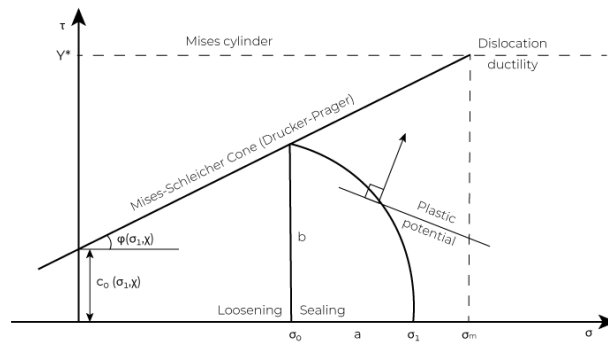

Fig. 1. Surface view of the limiting state of rocks

The main difficulty in describing the deformation beyond the elastic limit lies in the fact that the limiting surface is not fixed, it changes during deformation. On the loading diagrams, a hardening section is observed, where the increment of plastic deformation occurs with increasing stresses, followed by stress relief, and destruction occurs. In the course of deformation, not only the limiting surface changes, but also the ratio between the increments of the shear and volume parts of plastic deformation,

i.e., the direction of the plastic deformation vector. Thus, parameters describing the behavior of the rock beyond the elastic limit become accumulated plastic deformation and pressure functions.

It should be noted that the hardening section on the loading diagram in such media is very difficult to interpret. Formally, strength is described by two parameters: adhesion and internal friction. However, geometric causes contribute to effective hardening. Dilatancy hardening [12, 13] is especially evident in cramped conditions of deformation, when an increase in volume leads to an increase in pressure. This phenomenon is of particular importance in geomechanical processes. It was shown in [14] that an increase in the effective strength of the sample can be observed even with a slight decrease in the adhesion.

3   Parallel architecture

There are two different approach in multicore parallel computing - Shared memory parallelization and Distributed memory parallelization:

- Shared memory parallelization(SIMD) - architecture where each processors using the main memory for communicating of data. OpenMP is a main platform shared memory architecture. OpenMP is a simple instruction to divide a process into some subprocess which are called threads. OpenMP using in many programming language such as C/C++ and Fortran.
- Distributed memory parallelization(MIMD) - architecture where each processors has own local memory which are called nodes. All nodes connected in one communication network. Each node will execute the code and working with data using own local memory. Then, final result should be distributed to the main(master) node to gather all results. To work with this architecture is used MPI (Message Passing Interface). MPI have implementation in programming languages C/C++ and Fortran and other.

In addition to the two main platforms OpenMP and MPI, there is a hybrid platform - OpenMPI, which uses the capabilities of both plotforms. In addition to OpenMPI, there is also a full-fledged language for parallel programming of hybrid architectures - Unified Parallel C.

Also in OpenMP, in addition to the built-in functions for parallelizing calculations, the built-in capabilities of the processor for parallelization, the so-called Math Kernel Library(MKL), are used. MCL can compute operations of addition, subtraction and multiplication over vectors and matrices in parallel.

The parallel speedup can be obtained by:

$$S(p) = \frac{T_1}{T_p} \tag{18}$$

Where:

— $S(p)$ is speedup by using parallel programming using p processor,
— T_1 the CPU time by using single processor,
— T_p CPU time by using p processor.

The parallel efficiency can be obtained by:

$$E = \frac{S(p)}{p} \times 100\% \tag{19}$$

In the process of coal mining in the bottom, the boundary of the zone of inelastic deformations moves deep into the massif, which increases the number of calculations during the simulation, and the acceleration of simulation of this process will make it possible to obtain data much faster and more accurately due to an increase in the size grid.

The solution of the system of equations is carried out on the computational grid, which covers the studied region of the medium or the entire sample, the discretization of the computational region is carried out. On the constructed computational grid, all functions are approximated and a system of equations is solved. Of course, difference schemes that have been successfully used for many years, either for problems in the deformation of the geomedium, are described in detail in [15, 16]. The standard features of numerical calculation are used, which are implemented in original software packages.

The OpenMP program is simple, for instance in C++, the instruction only add syntax "#pragma omp parallel for" above the looping codes, then, the single core will automatically divide the loop into several block.
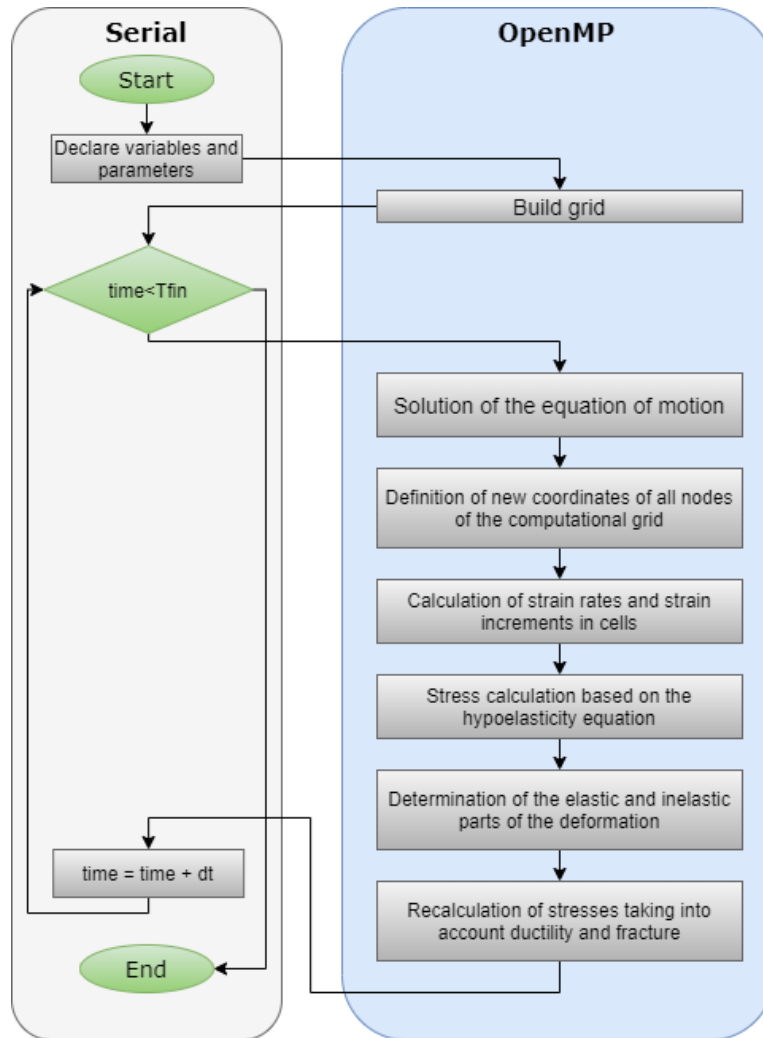
Fig. 2. Block process of OpenMP architecture

The MPI program in Fig. 3 has two domains of computation. The difference part from block process of OpenMP is located on looping time. Other processors will be executed time loop similar to the master.

In MPI, each processors need communication to each other for transferring data from master to slave. MPI have commands "`MPI_Send()`" and "`MPI_Recv()`" to send and receive data. But MPI (MIMD architecture) needs more communication time than the SIMD architecture and MPI could not guarantee produces best execution time.
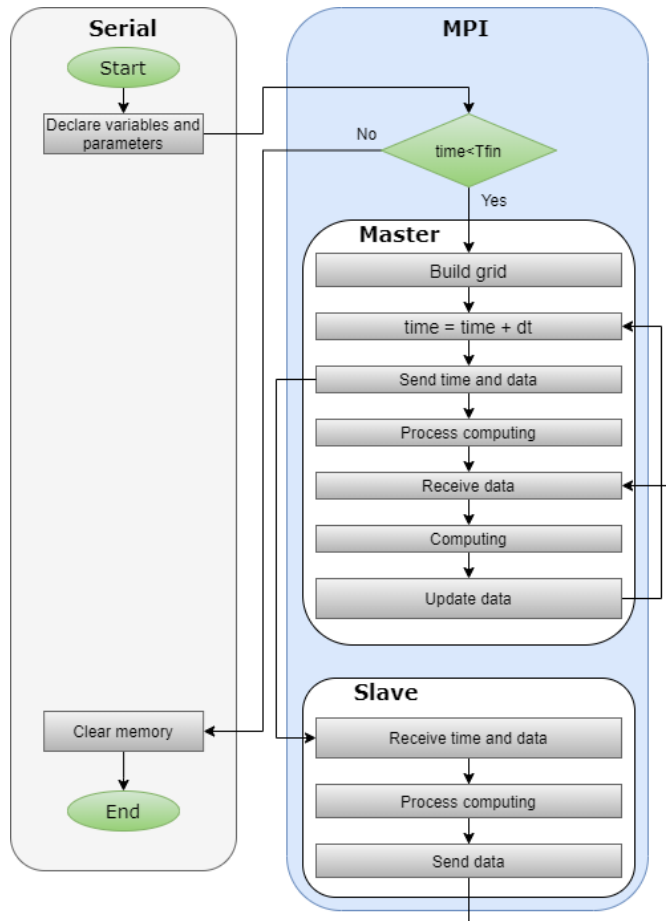
Fig. 3. Block process of MPI architecture

4 Experiments and results

To obtain simulation results and parallel performance, the following computer specifications are used.

Table 1. The Computer Specifications

Name	Type
Operating system	CentOS 6
Processors	Intel Xeon X5560 2.8 GHz
RAM	16GB
CPU(s)	16

The performance of MPI and OpenMP will be elaborated. The runtime for MPI and OpenMP for simulation is done for 10 seconds of the process.

Table 2. Computing time

Number of grid	Serial (s)	Time (s) of OpenMP		Time (s) of MPI	
		8 cores	16 cores	8 cores	16 cores
200	27.8096	49.5230	61.9437	36.8255	54.3485
400	94.8357	110.2547	99.3012	82.2647	135.8475
800	370.5342	245.9861	240.1843	237.1254	330.1293
1600	1490.5422	690.5362	580.1232	740.9543	997.3753

Table 2 shows the comparison of modeling time in serial parallel using 8 and 16 cores for each type. Form the Table 2, the modeling time in serial for number of grids 200 and 400 is smaller than the modeling time in parallel except MPI type for 8 cores. This means the parallel processing is not less efficient since the number of grid points is small, in this case using single core is already enough. However, using the large number of points (from 800 and greater), the modeling time in parallel is better than the serial.

From Table 2, the speedup (18) and efficiency (19) performances of OpenMP and MPI using 8 and 16 cores can be achieved. The speedup and efficiency profiles are shown in Fig. 2 and 3 respectively. In Fig. 2, the speedup of OpenMP is better than MPI for different number of cores. However, the speedup using MPI shown slightly better in number of grids 800 8 cores. The MPI fails to get the good speedup performance due to the time for changing messages in processors is dominant than the computing time.
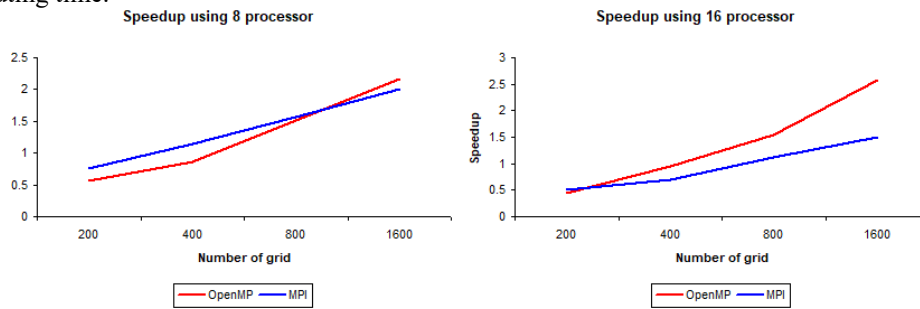

Fig. 4. Speedup of OpenMP and MPI using 8 (left) and 16 (right) cores.
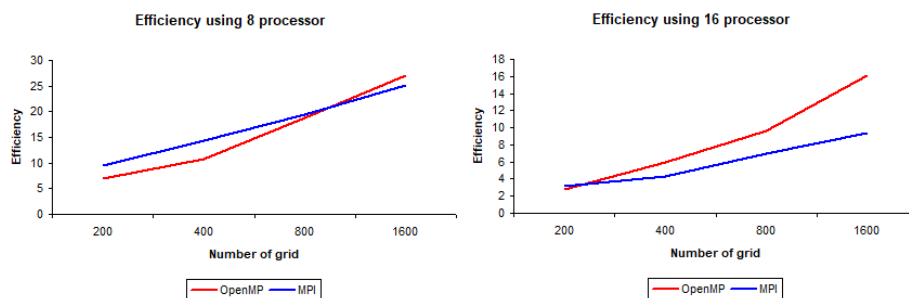
Fig. 5. Efficiency of OpenMP and MPI using 8 (left) and 16 (right) cores.

The efficiency profiles in Fig. 3 are given. The efficiency of parallel processing using 8 cores is better than 16 cores in both platforms.

5   Conclusion

Two parallel architectures OpenMP and MPI have been implemented for simulating the 2D deformation process. The results show the modeling time of OpenMP and MPI are better than the serial programming when the number of grids is more than 200 points.

References

1. Bobrov, I.V., Krichevskiy, R.M., Mihaylov, B.I.: Vnezapnyie vyibrosyi uglya i gaza na shahtah Donbassa, Ugletehizdat (1954)
2. Nikolin, V.I., Mordasov, V.I., Savchenko, P.I.: Obosnovanie minimalnogo chisla neschastnyih sluchaev, neobhodimyih dlya dostovernogo analiza travmatizma. In: Izvestiya Gornogo institute, vol. 2, pp. 41-44 (1999)
3. Ruppeneyt, K.V.: Nekotoryie voprosyi mehaniki gornyih porod, Ugletehizdat (1954)
4. Bridgmen, P. W.J.: Appl. Phys (1960)
5. Buzer, G.D., Hiller, K.H., Serdengekti, S.: Vliyanie porovoy zhidkosti na deformatsionnoe povedenie gornyih porod pri trehosnom szhatii. In: Mehanika gornyih porod, pp. 372-406 (1966)
6. Zabigaylo, V.E., Nikolin, V.I.: Vliyanie katageneza gornyih porod i metamorfizma ugley na ih vyibrosoopasnost, Naukova dumka (1990)
7. Bridzhmen, P.V.: Issledovanie bolshih plasticheskih deformatsiy razryivov, Izd-vo inostrannoy literaturyi (1955)
8. Levkin, N.B.: Predotvraschenie avariy i travmatizma v ugolnyih shahtah Ukrainyi, Donbass (2002)
9. Stefanov, Yu.P.: Chislennoe modelirovanie deformirovaniya i razrusheniya gornyih porod na primere rascheta povedeniya obraztsov peschanika. In: Fiziko-tehnicheskie problemyi razrabotki poleznyih iskopaemyih, vol. 1, pp. 73-83 (2008)
10. Stefanov, Yu.P.: Nekotoryie osobennosti chislennogo modelirovaniya povedeniya uprugohrupkoplastichnyih materialov. In: Fizicheskaya mezomehanika, vol. 8, pp. 129-142 (2005)

11. Uilkins, M.L.: Raschet uprugoplasticheskih techeniy. In: Vyichislitelnyie metodyi v gidrodinamike, pp. 212-263 (1967)
12. Nikolaevskiy, V.N.: Mehanicheskie svoystva gruntov i teoriya plastichnosti. In: Mehanika tverdyih deformiruemyih tel. Itogi nauki i tehniki, vol. 6, pp. 5-85 (1972)
13. Garagash, I.A., Nikolaevskiy, V.N.: Neassotsiirovannyie zakonyi techeniya i lokalizatsii plasticheskoy deformatsii. In: Uspehi mehaniki, vol. 12, pp. 131-183 (1989)
14. Stefanov, Yu.P.: Numerical investigation of deformation localization aгd crack formation in elastic brittle-plastic materials. In: J.Fract., vol. 128, pp. 345-352 (2004)
15. Wilkins, M.L.: Computer Simulation of Fracture. Lawrence Livermore Laboratory, Rept. UCRL-75246 (1972)
16. Wilkins, M.L.: Computer Simulation of Dynamic Phenomena, Berlin–Heidelberg–New York: Springer-Verlag (1999)